

Transient Absorption Spectroscopic Study on Band-Structure-Type Change in CdTe/CdS Core-Shell Quantum Dots

Lei Wang, Hai-Yu Wang, Bing-Rong Gao, Ling-Yun Pan, Ying Jiang, Qi-Dai Chen, Wei Han, and Hong-Bo Sun, *Member, IEEE*

Abstract—We report on the band edge alignment in zinc-blended-type CdTe/CdS core-shell quantum dots, using femtosecond spectroscopy. Time-resolved transient absorption spectroscopy directly shows that the system gradually developed from quasi-type-I to type-II as the shell thickness increased. Following photoexcitation of CdS, the injection of a hole from CdS valence band into CdTe valence band is observed. The hole transfer occurs on the 1000 fs time scale in these heteromaterials. Furthermore, a strain ca. 150 meV is obtained by comparing the transient with steady-state spectra.

Index Terms—Band structure, core-shell quantum dots, strain, transient absorption.

I. INTRODUCTION

SEMICONDUCTOR quantum dots (QDs) exhibit well-known quantization behaviors owing to the local motion confinement of electrons [1]. As a test-bed for fundamental physics and photonic applications on the nanoscale, numerous works have been focused on size-dependent optical, electronic properties, and multiexciton relaxation time [2]–[4]. For example, colloidal semiconductor QDs exhibit wide potential for single-photon source of quantum communication, broadband absorption solar cells, and fluorescent labels in biology and biomedicine [5]–[7]. Of late, the core-shell nanostructures are providing another interesting opportunity to manipulate the band structures of QDs [8]. Different from planar quantum wells and superlattices [9]–[13], the quantized energy level distribution of the epitaxially grown core-shell QDs depends not only on the core-shell lattice mismatch, but also on the core size and shell thickness. This gives plenty of room for the band gap engineering of QD systems. In some cases, it could extend emission range from visible to near-infrared [14]. The

core-shell structure would also suggest a possible approach to inhibit fluorescence blinking, which could bring about a bright future in application [15].

There have been lots of explorations for well-defined core-shell heterostructures, such as type-I CdTe/ZnS and type-II CdTe/CdSe. These materials will mainly keep the bulk-type band structure at the interface between the two semiconductors, but with shift of band offset. An interesting case is type-I CdTe/ZnSe [8]; when the core CdTe size is small (3.5 nm), it will gradually develop from type-I to type-II core-shell structure as the shell thickness increases, which is due to the enhanced quantum confinement and strain. If the CdTe core is large (7 nm), it will return to type-I, owing to a little strain as the shell exceeds a critical thickness. Another interesting case is CdTe/CdS core-shell QDs that have a considerably small band offset of electron. The interfacial band edge alignment in this system still remains controversial. CdTe/CdS was earlier known as type-I structure [16]–[18]. However, other researchers also considered it to be a type-II structure [8], [19]–[22]. Recently, in inverted CdS/CdTe QDs, the transition from quasi-type-II to type-I band offset was observed as the thickness of shell changed [23]. Can the type transition also happen in CdTe/CdS structure? Here, we have performed transient absorption (TA) experiments for water solution CdTe/CdS core-shell QDs (the diagrams of the heterostructure and bulk band offset are shown in Fig. 1), to address how the thickness of the shell affects the band offset as well as the band edge relaxation dynamics of charge carriers.

II. EXPERIMENTAL

A. Materials, Steady-State Properties, X-Ray Diffraction, and High-Resolved Transmission Electron Microscopy

The water solution CdTe/CdS core-shell QDs are synthesized by a modified literature method, but the CdTe core is smaller [17]. Typically, for CdTe core QDs, 1 mM of CdCl₂·2.5H₂O solution and 2 mM of 3-mercaptopropionic acid (MPA) were mixed, and the pH of the solution was adjusted to about 11 by dropwise addition of 1 M NaOH solution with stirring. Then under N₂ protection, 0.2 mmol of NaHTe solution were added at room temperature. So the ratio of Cd:MPA:Te in the reaction solution was 1:2:0.2. Usually, when its absorption peak appeared at about 460 nm after the reflux temperature reached 100 °C, the desired core was prepared. Then, when the core solution was cooled down, 1 mM

Manuscript received March 25, 2011; revised June 7, 2011; accepted June 11, 2011. Date of current version July 19, 2011. This work was supported in part by the National Natural Science Foundation of China, under Grant 20973081, Grant 60525412, Grant 60677016, Grant 61076054, and Grant 10904049.

L. Wang, B.-R. Gao, Y. Jiang, and Q.-D. Chen are with the State Key Laboratory for Integrated Optoelectronics, College of Electronic Science and Engineering, Jilin University, Changchun 130012, China.

H.-Y. Wang and H.-B. Sun are with the State Key Laboratory for Integrated Optoelectronics, College of Electronic Science and Engineering, Jilin University, Changchun 130012, China. They are also with the College of Physics, Jilin University, Changchun 130023, China (e-mail: haiyu_wang@jlu.edu.cn; hbsun@jlu.edu.cn).

L.-Y. Pan and W. Han are with the College of Physics, Jilin University, Changchun 130023, China.

Color versions of one or more of the figures in this paper are available online at <http://ieeexplore.ieee.org>.

Digital Object Identifier 10.1109/JQE.2011.2159853

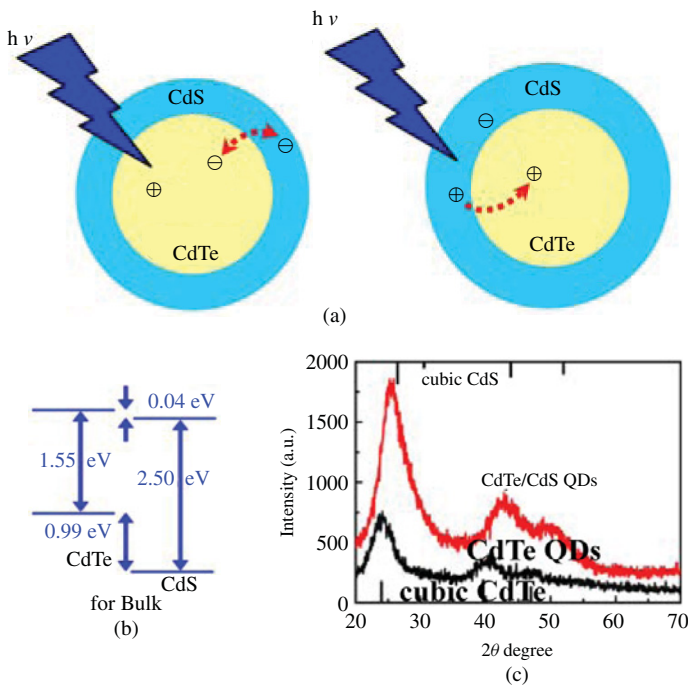


Fig. 1. (a) Simple diagram of experiments. Left: the case that CdTe core is excited. Right: the case that CdS shell is dominantly excited. (b) Schematic of band offsets for bulk materials. (c) XRD spectra of CdTe and CdTe/CdS QDs. The lines correspond to bulk cubic zinc blende CdTe (bottom) and cubic zinc blende CdS (top).

of thiourea solution (thiourea: Cd = 4:1) was added for the CdS shell growing at a pH of about 11. After degassing at room temperature, the reaction solution was heated to 100 °C under N_2 protection, and then was timed. At a different time, the desired CdTe/CdS core-shell QDs could be obtained (namely from S1 to S4, respectively). We also check out a “blank” experiment, where only the core material is absent. The result indicates that CdS QDs could not exist alone. The steady-state absorption spectra were measured using a Shimadzu UV-1700 spectrophotometer. The steady-state fluorescence spectra were recorded with a Shimadzu RF-5301PC spectrometer. Power X-ray diffraction (XRD) patterns were recorded on a Rigaku D/max-rA diffractometer using Cu $K\alpha$ radiation. The high-resolution transmission electron microscopy (HRTEM) images were obtained with a JEOL-2100F field emission TEM.

B. Time-Correlated Single-Photon Counting

Nanosecond fluorescence lifetime experiments were performed by the time-correlated single-photon counting (TCSPC) system under right-angle sample geometry. A 405 nm picosecond diode laser (Edinburgh Instruments EPL375, repetition rate 2 MHz) was used to excite the samples. The fluorescence was collected by a photomultiplier tube (Hamamatsu H5783p) connected to a TCSPC board (Becker&Hickel SPC-130). Time constant of the instrument response function (IRF) is about 500 ps.

C. Transient Absorption Measurement

A transient absorption system [24] was performed to further investigate the possible type transition for these samples. The

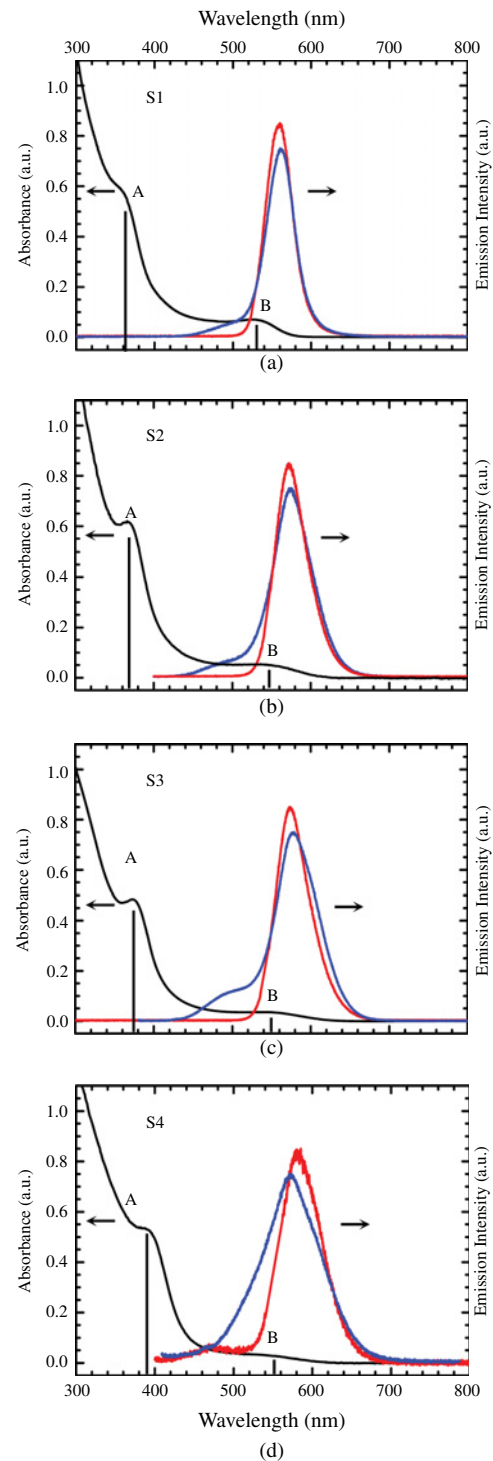


Fig. 2. Steady-state absorption (black line) and emission spectra of CdTe/CdS core-shell samples. Red line represents the excitation at band edge absorption peak (B-band). Blue line represents the excitation at absorption peak (A-band).

TA setup consisted of 400 nm pump pulses doubled from 800 nm laser pulses (~ 100 fs duration, 250 Hz repetition rate) generated from a mode-locked Ti:sapphire laser/amplifier system (Spectra-Physics) and broadband (350-700 nm) white-light probe pulses generated from 5-mm-thick CaF_2 substrate. The relative polarization of the pump and the probe beams was set to the magic angle. To avoid degrading, the sample

TABLE I
AVERAGE SIZE OF SAMPLES FROM TEM DATA AND DIFFERENCE
BETWEEN STEADY-STATE AND TRANSIENT SIGNALS

	Average Size (nm)	Shell Coverage (ML)	Steady-state Peak of CdS (nm)	Transient Signal of CdS (nm)	ΔE_{S-T} (meV)
S1	2.3	0.3	360	363	28
S2	2.5	0.6	368	388	174
S3	2.7	1.0	375	395	167
S4	3.2	1.6	390	407	133

was placed in a 0.5-mm-thick quartz cell cycle flowing by a micro pump. Before and after experiments, we measured the absorption spectra of samples, and no obvious change was observed. The TA data were collected by a fiber-coupled spectrometer connected to a computer. The group velocity dispersion of the transient spectra was compensated by a chirp program. To obtain the same relative delay across the entire spectrum, the zero point of signals in time axis at each wavelength is calibrated. After satisfied fitting the dispersion curve, this correction is automated by computer.

III. RESULTS AND DISCUSSION

A. Steady-State Photophysical Properties, XRD, and HRTEM

Similar to other core-shell systems [25], [26], it seems that the steady-state absorption spectra are the superposition of absorbance of CdS QDs and CdTe QDs (Fig. 2), due to the low oscillator strength of indirect transition between the two materials. All samples exhibit two absorption bands (A and B), which correspond to the lowest energy 1S transitions of CdS and CdTe, respectively. As the shell grows, A-band becomes more pronounced and shows a red shift (from ~ 360 nm to ~ 390 nm); the band edge absorption (B-band) is broadening and also has a red shift (from ~ 530 nm to ~ 550 nm), which indicates that the samples S3 and S4 have a behavior of type-II core-shell nanostructures [8], [20], [26]. This also excludes the case of the alloy, which leads to a blue shift in absorption and emission, and implies that type-I to type-II transition may occur when the coverage or thickness of the shell increases. If the band edges of samples are excited, the dominant emission peaks locate at 560 nm, 570 nm, 574 nm, and 585 nm from S1 to S4, respectively (red line in Fig. 2). When the A-band of samples is excited, a shoulder appears at the blue side of the PL peak, and the ratio of shoulder increases as the shell grows (blue line in Fig. 2). Usually, the surface of CdS is not well passivated in water, and the thick shell layer of CdS may induce new interface traps that are similar to the CdSe/CdTe system [27]. So, these emissions are very likely due to these traps, the level of which are located between the valence band minimum of CdTe and CdS as a hole trap.

The XRD patterns of CdTe and CdTe/CdS QDs are presented in figure 1(c). Our result shows that CdTe/CdS QDs are still zinc blended structures, which is consistent with the characteristic cubic zinc blende CdTe bulk material and CdTe QDs patterns. But in comparison with the bare CdTe QDs, the diffraction peaks of CdTe/CdS QDs trend to the location of cubic CdS phase. This indicates the shell effect

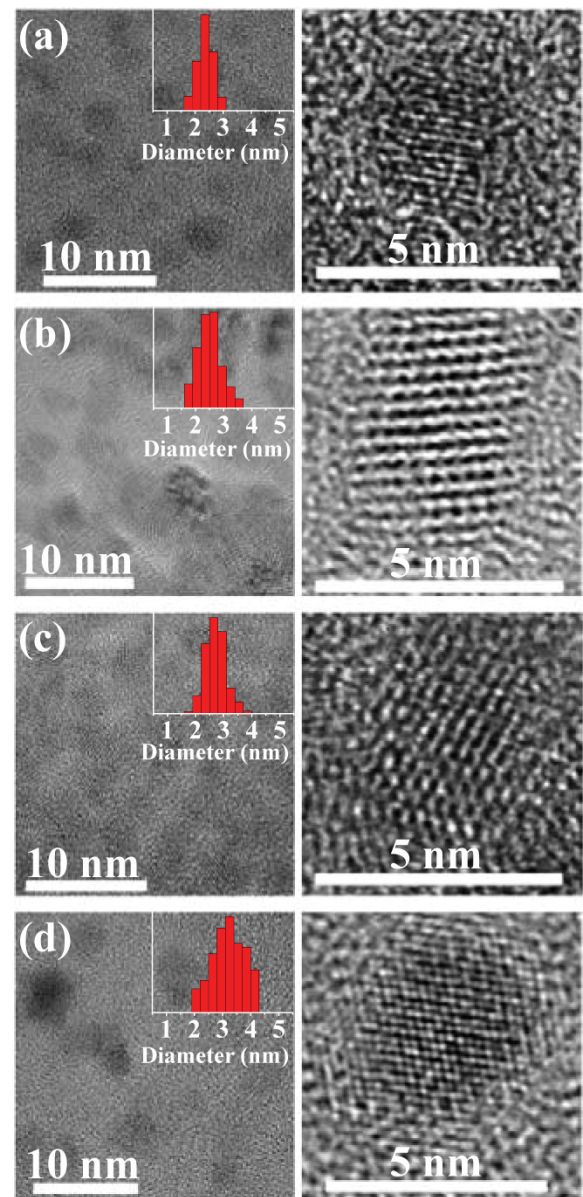


Fig. 3. HRTEM images of all CdTe/CdS core-shell samples. Insets are the size distributions.

on the core lattice. As per Nie's point, because of the lattice mismatch between CdTe and CdS, a CdS shell will compress a CdTe nanocrystal and further result in a change in the energy band offsets [8]. However, at present it is far from clear. Detailed theoretical studies on the role of strain are few [28]. A quantitative debate about this effect still keeps on. This problem in our case is discussed later, according to our steady-state and transient experimental results.

Figure 3 shows the HRTEM images of all core-shell samples. The average size is 2.3 nm, 2.5 nm, 2.8 nm, and 3.2 nm from S1 to S4, respectively. Because the average size of CdTe core is about 2.1 nm (not shown here) and the thickness of 1 monolayer (ML) CdS shell is estimated to be about 0.35 nm [29], the average shell coverage or thickness is 0.1 nm, 0.2 nm, 0.35 nm, and 0.55 nm, which means CdS shell grows by about 0.3 ML, 0.6 ML, 1.0 ML, and 1.6 ML,

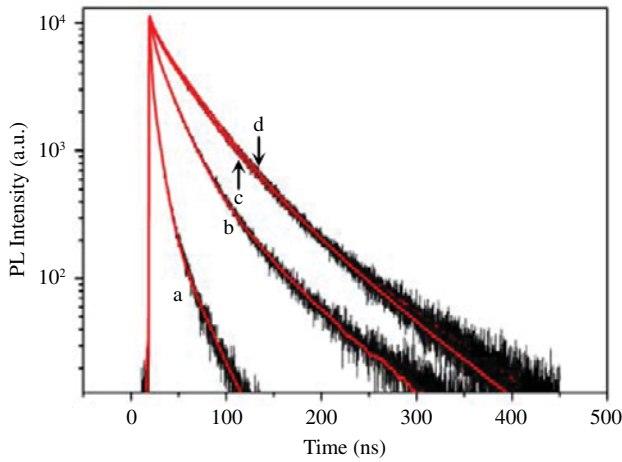


Fig. 4. Nanosecond fluorescence decay traces of (a) Core CdTe QD. (b) Reference plain CdTe QD. (c) S1, and (d) S3. Red line is the fitting curve.

respectively (all these data have been presented in Table I). It is noteworthy that the coverage of shell layer is imperfect for samples with average shell thickness < 1 ML.

B. Time-Correlated Single-Photon Counting

Fluorescence lifetime is an important parameter to characterize the inference of inorganic shells. We have carried out the time-resolved PL study by the TCSPC system.

Figure 4 shows the PL decay curves of two plain CdTe QDs and two core-shell samples, S1 and S3. For the plain CdTe QDs, one is the core CdTe QD and the other has a band edge absorption peak and PL peak near to S3, as a reference. All the fluorescence transients were well fitted with multiexponential functions; the best-fit parameters are listed in Table II. Although it is difficult to know the origin of each component, an apparent fact is that the average PL lifetime of core-shell samples is longer than that of plain CdTe QDs. This is usually due to the delocalization of electron to the shell or/and surface trap. Whatever be the case, our observation shows that the electron has larger probability in the shell of core-shell sample. On the other hand, the PL lifetime of core-shell slightly increases with the shell thickness in the range of 0.3 ML to 1.0 ML. From our perspective, it indicates that the charge separation has been increased with the shell thickness, if it is a result from the formation of type II structure. So, to further understand the photophysics, it is important to carry out TA spectroscopy study on these core-shell structure nanocrystals.

C. TA Spectroscopy

Ultrafast TA spectroscopic technology is a useful tool to study the heterostructure nanocrystals [22], [25], [30]. For CdTe/CdS system, it is difficult to make out the origin of emission in spectrum due to the small conduction band offset in transient PL. However, the large enough difference in band gap makes it easier to distinguish the character of each material in TA experiments. According to the steady-state absorption spectra, optical pump at 400 nm leads to different excitations.

TABLE II
FLUORESCENT LIFETIMES BY TCSPC

	τ_1 (ns)	τ_2 (ns)	τ_3 (ns)	τ_{av} (ns)
Core CdTe QD	1.3 (70.7%)	7.2 (26.6%)	27.3 (2.7%)	3.6
Reference CdTe QD	3.2 (38.2%)	19.2 (52.2%)	56.1 (9.6%)	16.6
S1	7.1 (19.3%)	34.6 (69.4%)	88.3 (11.3%)	35.4
S3	6.9 (18.0%)	35.9 (68.1%)	77.8 (13.9%)	36.5

For S1 and S2, only core CdTe is excited since the pump energy is below the band gap of CdS shell layer. As the absorption of the band gap of CdS shifts in, the shell will be predominantly excited in S3 and S4. This leads to different relaxation pathways of the charge carriers in the two kinds of samples. Figure 5 shows the temporal evolution of the TA spectra of these QDs, from which we can more clearly check out the difference between the four samples in detail. For S1, two bleaching peaks with maxima at 363 nm and 533 nm are in agreement with the steady-state absorption spectra (Fig. 5a). These signals can be assigned to CdS^- and CdTe_{15} states. Since CdS shell cannot be directly excited, CdS^- state is obviously due to the electron filling from CdTe. For S2, the transient behavior is similar to S1 (Fig. 5b). However, although the bleaching peak corresponding to CdTe_{15} state still matches with steady-state spectra, the signal to CdS^- state begins to shift red more than one hundred meV (seen Table I) after carefully examining the spectra, excluding the possibility of experimental errors. For S3 and S4, both TA spectra show the dominant state-filling signal of CdS_{15} , red-shifted when compared to the location of steady-state peak, with a weak bleaching of CdTe^+ that results from the hole transfer for CdS shell (Fig. 5c and 5d). In TA experiments about QDs, the red shift of bleaching usually comes from the superposition with the stimulated emission. However, as shown in steady-state spectra, the emission is far away from the bleaching signal of CdS, so we rule out this case. Another considerable effect is the interfacial strain. As mentioned earlier, the shell layer of CdS will increase the band gap of the CdTe core, while the band gap of shell material will decrease. As is known, the quantum confinement effect will decrease as the size increases, which will decrease the band gap of materials. This means that in CdTe/CdS core-shell nanocrystals, there is a competition between quantum confinement and strain for core, and an additional effect to decrease the band gap due to strain for shell. Our observation from the TA spectra consists of the latter. So, we suggest that the interfacial strain already exists even in the shell thickness < 1 ML, and the red shift of CdS bleaching signal results from the interfacial strain. At last, as a comparison, we examine pure CdTe QDs with similar band edge absorption peak to S3, where only the bleaching of CdTe_{15} transition is observed (Fig. 5e).

Based on the ratio of bleaching amplitude of the CdS and CdTe band, we can estimate the value of the band offset of

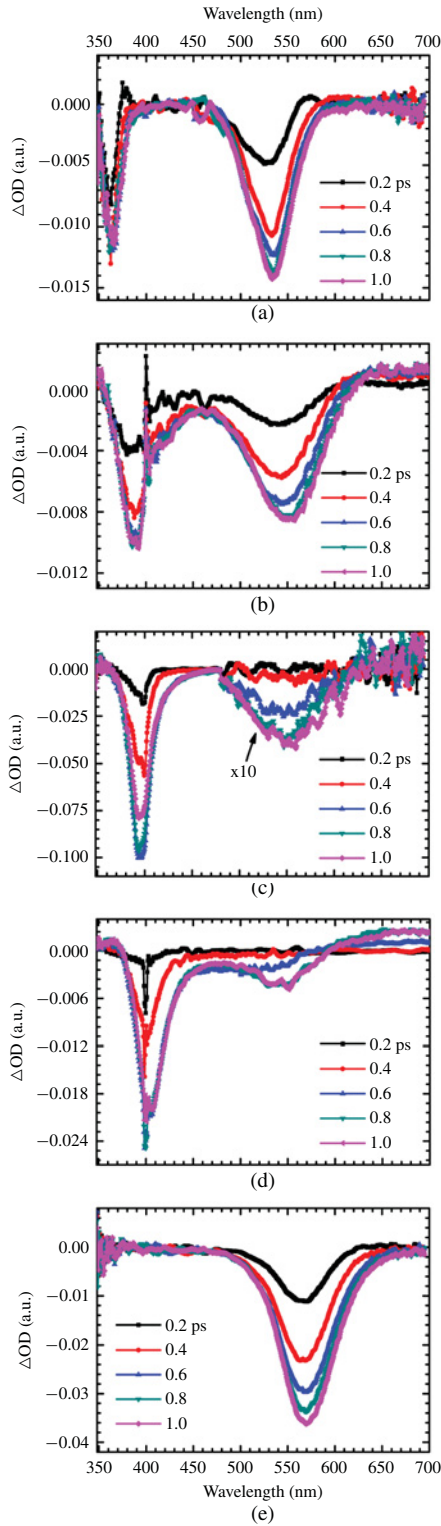


Fig. 5. TA spectra of (a) CdTe/CdS core-shell sample S1. (b) S2. (c) S3. (d) S4. (e) Only CdTe following 400 nm photoexcitation.

electron. For the thin shell (coverage less than one monolayer) samples S1 and S2, the ratio of the oscillation strength of CdS and CdTe band is about 5, according to the steady-state absorption spectra (for CdS band edge absorption, the contribution from CdTe is subtracted). So, when the states of

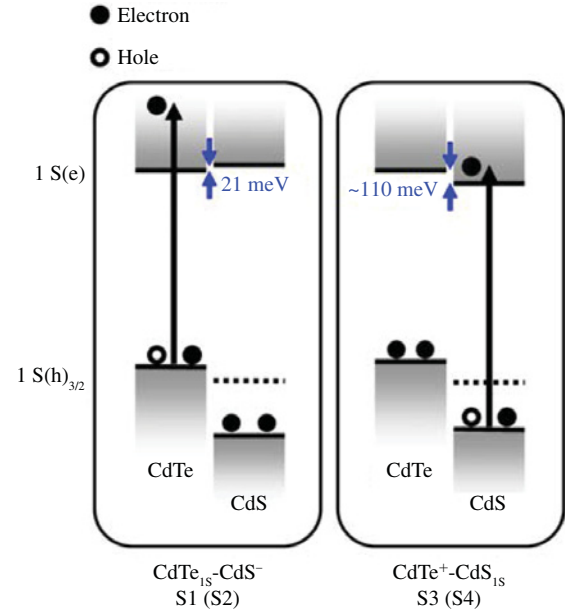


Fig. 6. Band edge alignment in S1 (S2) and S3 (S4) (left and right). The arrows indicate the excitation. The dot lines represent the trap level in these systems.

CdS and CdTe are equally populated, the bleach signal of CdS will be about five times that of CdTe. Our result shows that the ratio is about 0.8 (Fig. 5a). Taking into account that the bleaching signal is the sum of electron and hole contributions, we can get the following equations by taking advantage of the principle of detail balance:

$$\frac{5 \times N_e^{CdS}}{N_e^{CdTe} + N_h^{CdTe}} = 0.8, \quad N_e^{CdS} + N_e^{CdTe} = N_h^{CdTe},$$

$$\frac{N_e^{CdS}}{N_e^{CdTe}} = \exp\left(\frac{-\Delta E}{k_B T}\right)$$

where N_e and N_h are the populations of electron and hole, respectively; ΔE is the band offset between CdS and CdTe; k_B is Boltzmann constant; and T is temperature. At room temperature $k_B T$ is equal to 25 meV, we can obtain the band offset as about 21 meV. This small offset will result in the delocalization of the electron, so the samples S1 and S2 have a quasi-type-I structure. In contrast, for the samples S3 and S4, the ratio of the bleach signals is about 20; it implies that almost all the electron population is located in the shell, while the small bleach signal of CdTe is contributed by its hole. This is a typical behavior of type-II structure. In fact, the CdS-band shifts by about 181 meV from sample S1 to S3, the shift of the electron level will be around 135 meV since the ratio of effective mass of electron and hole is about 3 for CdS QDs [23], [26]. It will change the electron offset to ~ 110 meV if the band of the CdTe-core remain the same. At room temperature, one can expect nearly no electron population in the core, which is consistent with our observation. From this point of view, the optical transitions and possible states are illustrated in figure 6.

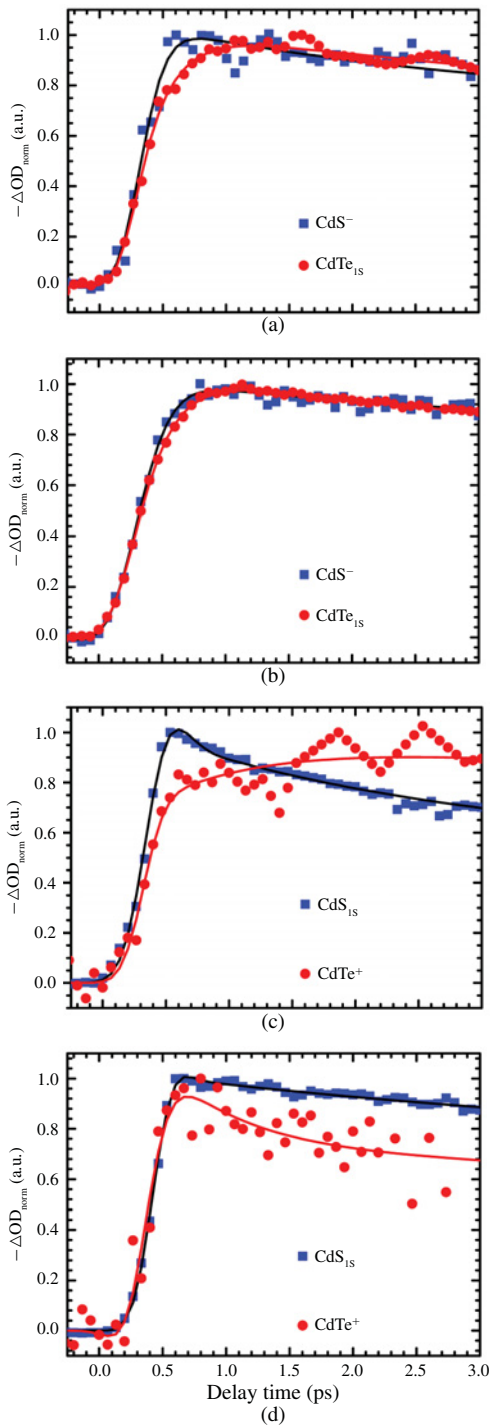


Fig. 7. Kinetics of (a) CdTe_{1S}-CdS⁻ and (b) CdTe⁺-CdS_{1S} state-filling signals during the first 3 ps following photoexcitation in S1, S2, S3, and S4, respectively.

D. Transient Carrier Dynamics

Finally, by extracting the dynamics of these states from the TA spectrum (Fig. 7), the state filling process can be resolved. Using multiexponential fitting, we find that the filling time of CdS⁻ is almost instantaneous (< 100 fs), which is faster than the time constant of CdTe_{1S} (~ 240 fs) in S1 and S2 (Fig. 7a and 7b). This indicates that the hot electron relaxation

to the shell is easier, which agrees with the statement that conduction band minimum (CBM) of CdS is a little higher than the CBM of CdTe. Therefore, S1 and S2 are indeed a quasi-type-I structure. Another feature is that the filling time trends to be slow for CdS⁻ state as the shell coverage increases from 0.3 ML to 0.6 ML, while the filling time of CdTe_{1S} state almost stays the same in the first two samples, though the size is increasing. It further matches with the case mentioned earlier that there is an interfacial strain, by which the core and shell have different transient behaviors. On the other hand, in the case of the latter two samples S3 and S4, due to the band edge excitation, a pair of electron and hole is instantaneously generated in the CdS shell. According to the results cited earlier, we can predict that a hole transfers to the core after shell excitation, generating a new state CdTe⁺. As shown in figure 7c, one clearly sees a slow filling of CdTe⁺ accompanied by a decay of the bleaching signals of CdS_{1S} in S3. The fitting result gives a time constant ~ 1000 fs for this hole transfer process. In the case of S4, there is a fuller and thicker shell, but far from being perfect. More dangling bonds or traps may appear. This leads to a spectrally broad and long lifetime of excited-state absorption (“reverse” signal to bleaching) in the red side of the bleaching signal of CdS in transient experiment, which covers the signal area of core and is comparable with the small bleaching signal of CdTe⁺ state. The superposition results in a fast rising at the beginning and a reversal when delay time is in excess of 200 fs (Fig. 7d).

IV. CONCLUSION

Using ultrafast broadband TA spectroscopy, the self-charge-separation in CdTe/CdS core-shell QDs is observed. By extending TA spectrum to the range of ultraviolet, we simultaneously obtained the evolution of ultrafast charge transfer of both core and shell in this system. As the shell grows, the band offsets of the system are tunable. Core-shell QDs gradually developed from quasi-type-I to type-II, in contrast to the results in the case of bulk [16], [19]. In quantum wells, the component content plays an important role for band structure changing, in which a critical content determines the transition between type I and type II [11]. In our study presented here, there is also a critical shell thickness playing the same role in the self-assembly colloid CdTe/CdS core-shell structure quantum dots. When the shell is thin (coverage less than 0.6 ML), it is quasi-type-I, in which a hole is localized in the core, and an electron is delocalized in the whole nanocrystal; when the shell is thick enough (coverage more than 1 ML for a 2.1 nm CdTe core), it becomes type-II, in which a hole is localized in the core CdTe, while an electron is localized in the shell CdS. When exciting CdS shell at band edge, the photoinduced hole transfer from CdS to CdTe occurs with a filling time of ~ 1000 fs. This work could help further comprehend other photophysics in heterostructure nanocrystals, that is, interfacial strain. According to the difference between the steady state and transient state, we give an experimental value ca. 150 meV of strain in the CdTe/CdS core-shell QDs, comparable with the theoretical value in the CdSe/CdTe nanowire [28].

REFERENCES

- [1] A. J. Nozik, "Spectroscopy and hot electron relaxation dynamics in semiconductor quantum wells and quantum dots," *Annu. Rev. Phys. Chem.*, vol. 52, pp. 193–231, Oct. 2001.
- [2] H. Y. Wang, C. M. Donegá, A. Meijerink, and M. Glasbeek, "Ultrafast exciton dynamics in CdSe quantum dots studied from bleaching recovery and fluorescence transients," *J. Phys. Chem. B*, vol. 110, no. 2, pp. 733–737, Jan. 2006.
- [3] R. J. Ellingson, M. C. Beard, J. C. Johnson, P. R. Yu, O. I. Micic, A. J. Nozik, A. Shabaev, and A. L. Efros, "Highly efficient multiple exciton generation in colloidal PbSe and PbS quantum dots," *Nano Lett.*, vol. 5, no. 5, pp. 865–871, Mar. 2005.
- [4] D. Oron, M. Kazes, and U. Banin, "Multiexcitons in type-II colloidal semiconductor quantum dots," *Phys. Rev. B*, vol. 75, no. 3, pp. 035330-1–035330-7, Jan. 2007.
- [5] P. Michler, A. Kiraz, C. Becher, W. V. Schoenfeld, P. M. Petroff, L. D. Zhang, E. Hu, and A. Imamoglu, "A quantum dot single-photon turnstile device," *Science*, vol. 290, no. 5500, pp. 2282–2284, Dec. 2000.
- [6] I. Gur, N. A. Fromer, M. L. Geier, and A. P. Alivisatos, "Air-stable all-inorganic nanocrystal solar cells processed from solution," *Science*, vol. 310, no. 5747, pp. 462–465, Oct. 2005.
- [7] M. Bruchez, Jr., M. Moronne, P. Gin, S. Weiss, and A. P. Alivisatos, "Semiconductor nanocrystals as fluorescent biological labels," *Science*, vol. 281, no. 5385, pp. 2013–2015, Sep. 1998.
- [8] A. M. Smith, A. M. Mohs, and S. Nie, "Tuning the optical and electronic properties of colloidal nanocrystals by lattice strain," *Nature Nanotechnol.*, vol. 4, no. 1, pp. 56–63, Jan. 2009.
- [9] C. Lin, Y. L. Zhen, and A. Z. Li, "Study of AlGaAsSb/InGaAsSb strained quantum well grown by molecular beam epitaxy on GaSb(100)," *Mater. Sci. Eng. B*, vol. 75, nos. 2–3, pp. 170–173, Jun. 2000.
- [10] K. Ohdaira, H. Murata, S. Koh, M. Baba, H. Akiyama, R. Ito, and Y. Shiraki, "Control of type-I and type-II band alignments in AlInAs/AlGaAs self-assembled quantum dots by changing AlGaAs compositions," *Phys. E*, vol. 21, nos. 2–4, pp. 308–311, Mar. 2004.
- [11] H. Grüning, P. J. Klar, W. Heimbrod, S. Nau, B. Kunert, K. Volz, W. Stolz, and G. Weiser, "Evidence for a type I to type II transition in (Ga, In)(N, As)/Ga(N, As) quantum well structures," *Phys. E*, vol. 21, nos. 2–4, pp. 666–670, Mar. 2004.
- [12] C. Schlichenmaier, H. Grüning, A. Thränhardt, P. J. Klar, B. Kunert, K. Volz, W. Stolz, W. Heimbrod, T. Meier, S. W. Koch, J. Hader, and J. V. Moloney, "Type I-type II transition in InGaAs–GaNAs heterostructures," *Appl. Phys. Lett.*, vol. 86, no. 8, pp. 081903-1–081903-3, Feb. 2005.
- [13] K. Hantke, J. D. Heber, C. Schlichenmaier, A. Thränhardt, T. Meier, B. Kunert, K. Volz, W. Stolz, S. W. Koch, and W. W. Rühle, "Time-resolved photoluminescence of type-I and type-II (GaIn)As/Ga(NAs) heterostructures," *Phys. Rev. B*, vol. 71, no. 16, pp. 165320-1–165320-9, Apr. 2005.
- [14] Z. T. Deng, O. Schulz, S. Lin, B. Q. Ding, X. W. Liu, X. X. Wei, R. Ros, H. Yan, and Y. Liu, "Aqueous synthesis of zinc blende CdTe/CdS magic-core/thick-shell tetrahedral-shaped nanocrystals with emission tunable to near-infrared," *J. Amer. Chem. Soc.*, vol. 132, no. 16, pp. 5592–5593, Apr. 2010.
- [15] T. D. Krauss and J. J. Peterson, "Bright future for fluorescence blinking in semiconductor nanocrystals," *J. Phys. Chem. Lett.*, vol. 1, no. 9, pp. 1377–1382, Apr. 2010.
- [16] D. W. Niles and H. Höchst, "Band offsets and interfacial properties of cubic CdS grown by molecular-beam epitaxy on CdTe(110)," *Phys. Rev. B*, vol. 41, no. 18, pp. 12710–12719, Jun. 1990.
- [17] Z. Y. Gu, L. Zou, Z. Fang, W. H. Zhu, and X. H. Zhong, "One-pot synthesis of highly luminescent CdTe/CdS core/shell nanocrystals in aqueous phase," *Nanotechnology*, vol. 19, no. 13, pp. 135604-1–135604-7, Feb. 2008.
- [18] D. Dorfs, T. Franzl, R. Osovsky, M. Brumer, E. Lifshitz, T. A. Klar, and A. Eychmuller, "Type-I and type-II nanoscale heterostructures based on CdTe nanocrystals: A comparative study," *Small*, vol. 4, no. 8, pp. 1148–1152, Aug. 2008.
- [19] S. H. Wei, S. B. Zhang, and A. Zunger, "First-principles calculation of band offsets, optical bowings, and defects in CdS, CdSe, CdTe, and their alloys," *J. Appl. Phys.*, vol. 87, no. 3, pp. 1304–1311, Feb. 2000.
- [20] Q. H. Zeng, X. G. Kong, Y. J. Sun, Y. L. Zhang, L. P. Tu, J. L. Zhao, and H. Zhang, "Synthesis and optical properties of type II CdTe/CdS core/shell quantum dots in aqueous solution via successive ion layer adsorption and reaction," *J. Phys. Chem. C*, vol. 112, no. 23, pp. 8587–8593, May 2008.
- [21] O. Schöps, N. Le Thomas, U. Woggon, and M. V. Artemyev, "Recombination dynamics of CdTe/CdS core-shell nanocrystals," *J. Phys. Chem. B*, vol. 110, no. 5, pp. 2074–2079, Jan. 2006.
- [22] S. Rawalekar, S. Kaniyankandy, S. Verma, and H. N. Ghosh, "Ultrafast charge carrier relaxation and charge transfer dynamics of CdTe/CdS core-shell quantum dots as studied by femtosecond transient absorption spectroscopy," *J. Phys. Chem. C*, vol. 114, no. 3, pp. 1460–1466, Jan. 2010.
- [23] Y. Nonoguchi, T. Nakashima, and T. Kawai, "Tuning band offsets of core/shell CdS/CdTe nanocrystals," *Small*, vol. 5, no. 21, pp. 2403–2406, Nov. 2009.
- [24] Y. Jiang, H.-Y. Wang, L.-P. Xie, B.-R. Gao, L. Wang, X.-L. Zhang, Q.-D. Chen, H. Yang, H.-W. Song, and H.-B. Sun, "Study of electron-phonon coupling dynamics in Au nanorods by transient depolarization measurements," *J. Phys. Chem. C*, vol. 114, no. 7, pp. 2913–2917, Feb. 2010.
- [25] C. J. Dooley, S. D. Dimitrov, and T. Fiebig, "Ultrafast electron transfer dynamics in CdSe/CdTe donor-acceptor nanorods," *J. Phys. Chem. C*, vol. 112, no. 32, pp. 12074–12076, Jul. 2008.
- [26] A. Nemchinov, M. Kirsanova, N. N. Hewa-Kasakarage, and M. Zamkov, "Synthesis and characterization of type II ZnSe/CdS core/shell nanocrystals," *J. Phys. Chem. C*, vol. 112, no. 25, pp. 9301–9307, Jun. 2008.
- [27] M. Jones, S. Kumar, S. S. Lo, and G. D. Scholes, "Exciton trapping and recombination in type II CdSe/CdTe nanorod heterostructures," *J. Phys. Chem. C*, vol. 112, no. 14, pp. 5423–5431, Mar. 2008.
- [28] S. Y. Yang, D. Prendergast, and J. B. Neaton, "Strain-induced band gap modification in coherent core/shell nanostructures," *Nano Lett.*, vol. 10, no. 8, pp. 3156–3162, Jul. 2010.
- [29] J. J. Li, Y. A. Wang, W. Z. Guo, J. C. Keay, T. D. Mishima, M. B. Johnson, and X. G. Peng, "Large-scale synthesis of nearly monodisperse CdSe/CdS core/shell nanocrystals using air-stable reagents via successive ion layer adsorption and reaction," *J. Amer. Chem. Soc.*, vol. 125, no. 41, pp. 12567–12575, Sep. 2003.
- [30] C. H. Chuang, S. S. Lo, G. D. Scholes, and C. Burda, "Charge separation and recombination in CdTe/CdSe core/shell nanocrystals as a function of shell coverage: Probing the onset of the quasi type-II regime," *J. Phys. Chem. Lett.*, vol. 1, no. 17, pp. 2530–2535, Aug. 2010.



Lei Wang received the B.S. degree from the College of Physics, Jilin University, Changchun, China, in 2008. He is currently pursuing the D.S. degree in the same university.

His current research interests include ultrafast photoelectronic conversion mechanism of organic molecules, nanocrystals, and artificial periodic micro-nano structures.



Hai-Yu Wang received the B.S. degree in physics from Jilin University, Changchun, China, in 1989, and the Ph.D. degree from Changchun Institute of Optics, Fine Mechanics and Physics, Chinese Academy of Sciences, Changchun, in 2000.

He worked as a Post-Doctoral Researcher at the University of Amsterdam, Amsterdam, the Netherlands, Ohio University, Athens, and the Arizona State University, Tempe, from 2001 to 2008. He joined Jilin University as one of the academic leaders at the end of 2008. He is currently a Full Professor at Jilin University. He has published over 30 scientific papers in well-known international academic journals such as *Science*, *the Proceedings of the National Academy of Sciences*, and *the Journal of the American Chemical Society*. His current research interests include understanding the nature of elementary dynamics in artificial complex and biological systems such as electron transfer, energy transfer, and other excited-state processes by ultrafast laser spectroscopy.



Bing-Rong Gao received the B.S. degree from the Department of Modern Physics, University of Science and Technology of China, Hefei, China, in 1999, and the M.S. degree from the Department of Geophysics, Peking University, Beijing, China, in 2002.

She is currently an Engineer in Jilin University, Changchun, China. Her current research interests include the study of photophysical properties of small organic molecules and polymers by time-resolved spectroscopy.



Ling-Yun Pan received the Ph.D. degree from the Department of Chemistry, Kwansai Gakuin University, Nishinomiya, Japan, in 2007.

She is currently a Teacher at Jilin University, Changchun, China. Her current research interests include exciton dynamics and nonlinear optical properties of self-assembled semiconductor nanostructures.



Ying Jiang received the B.S. degree in electronic information engineering science and the M.S. degree in electronics and systems from the College of Electronic Science and Engineering, Jilin University, Changchun, China, in 2008 and 2010, respectively. She is currently pursuing the D.S. degree in the same university.

Her current research interests include ultrafast photophysical processes of fluorescent molecules in solution as well as thin films and plasmon-exciton coupling interaction on metal nanostructures.



Qi-Dai Chen received the B.S. degree in physics from the University of Science and Technology of China, Hefei, China, in 1998, and the Ph.D. degree from the Institute of Physics, Chinese Academy of Sciences, Beijing, China, in 2004.

He was a Post-Doctoral Researcher at Osaka City University, Osaka, Japan, from 2005 to 2006. He is currently an Associate Professor at Jilin University, Changchun, China. His current research interests include laser microfabrication, ultrafast laser spectroscopy, photochemistry, and photophysics.



Wei Han received the B.S. degree in the Department of Physics, Jilin University, Changchun, China, in 1989, and the Ph.D. degree from Tomsk Polytechnic University, Tomsk, Russia, in 1997.

He is currently a Full Professor at Jilin University. He has published over 20 scientific papers in different academic journals and holds more than 25 Chinese patents. His current research interests include the preparation and application of nanomaterials in the field of energy and environment.



Hong-Bo Sun (M'99) received the B.S. and Ph.D. degrees in electronics from Jilin University, Changchun, China, in 1992 and 1996, respectively.

He worked as a Post-Doctoral Researcher in the Satellite Venture Business Laboratory, University of Tokushima, Tokushima, Japan, from 1996 to 2000, and then as an Assistant Professor in the Department of Applied Physics, Osaka University, Osaka, Japan. Since 2005, he has been a Full Professor at Jilin University. He was a Project Leader of the Precursory Research for Embryonic Science and Technology

Program, Japan, in 2001. He has published over 60 scientific papers in the below fields, which have been cited nearly 4000 times according to the Institute for Scientific Information search report. His current research interests include laser micro-nanofabrication, particularly in exploring novel laser technologies including direct writing and holographic lithography, and their applications on micro-optics, micromachines, microfluids, and microsensors.

Dr. Sun won the National Natural Science Funds for Distinguished Young Scholars, China, in 2005, and his team was supported by the Program for Changjiang Scholars and Innovative Research Teams at the Universities, in 2007. He was a recipient of the Award by the Optical Science and Technology Society for his contribution to the technology of femtosecond laser-initiated nanofabrication in 2002, and the Outstanding Young Scientist Award instituted by the Ministry of Education, Culture, Sports, Science and Technology, Japan, in 2006.